Technical Note

A non-invasive method to relate the timing of neural activity to white matter microstructural integrity

Steven M. Stufflebeam,[a,c,d] Thomas Witzel,[d] Szymon Mikulski,[b] Matti S. Hämäläinen,[a,c] Simona Temereanca,[a,c] Jason J.S. Barton,[e,f] David S. Tuch,[a,c,1] Dara S. Manoach,[b,c,]*

[a]Department of Radiology at the Massachusetts General Hospital and Harvard Medical School, Charlestown, MA 02129, USA
[b]Department of Psychiatry at the Massachusetts General Hospital and Harvard Medical School, Charlestown, MA 02129, USA
[c]Athinoula A. Martinos Center for Biomedical Imaging at the Massachusetts General Hospital and Harvard Medical School, Charlestown, MA 02129, USA
[d]Division of Health Sciences and Technology, Harvard Medical School and Massachusetts Institute of Technology, Cambridge, MA 02139, USA
[e]Department of Neurology, University of British Columbia, Vancouver, BC, Canada
[f]Department of Ophthalmology and Visual Sciences, University of British Columbia, Vancouver, BC, Canada

ARTICLE INFO

ABSTRACT

The neurophysiological basis of variability in the latency of evoked neural responses has been of interest for decades. We describe a method to identify white matter pathways that may contribute to inter-individual variability in the timing of neural activity. We investigated the relation of the latency of peak visual responses in occipital cortex as measured by magnetoencephalography (MEG) to fractional anisotropy (FA) in the entire brain as measured with diffusion tensor imaging (DTI) in eight healthy young adults. This method makes no assumptions about the anatomy of white matter connections. Visual responses were evoked during a saccadic paradigm and were time-locked to arrival at a saccadic goal. The latency of the peak visual response was inversely related to FA in bilateral parietal and right lateral frontal white matter adjacent to cortical regions that modulate early visual responses. These relations suggest that biophysical properties of white matter affect the timing of early visual responses. This preliminary report demonstrates a non-invasive, unbiased method to relate the timing information from evoked-response experiments to the biophysical properties of white matter measured with DTI.

© 2008 Elsevier Inc. All rights reserved.

Introduction

The neurophysiological basis of variability in the latency of evoked neural responses detected with electroencephalography (EEG) and magnetoencephalography (MEG) has been of interest for decades. A recently developed imaging technique, diffusion tensor imaging (DTI), can be used to investigate whether individual differences in the microstructural integrity of white matter tracts contributes to inter-individual variability in the timing of neural activity. White matter physiology, particularly myelination, has been proposed to contribute to individual differences in cognitive processing speed (e.g., Luciano et al 2004) based on the well-established role of myelin thickness and axon diameter in determining conduction velocity (Waxman, 1980). Recent reports of relations between DTI measures of fractional anistropy (FA) – an indirect measure of myelination (Harsan et al., 2006) and other WM microstructural properties (Beaulieu, 2002) – and cognitive reaction time support the proposal of a white matter contribution to variability in processing speed (Bucur et al., 2007; Gold et al., 2007; Madden et al., 2004; Manoach et al., 2007; Nestor et al., 2007; Tuch et al., 2005; Westerhausen et al., 2006). On this basis, we reasoned that WM microstructure might also contribute to the timing of evoked neural responses, which are a more direct measure of the timing of neural responses than behavior.

We investigated the relations of FA with individual differences in the latency of peak visual responses in occipital cortex as measured by MEG in the context of a saccadic paradigm. Using this paradigm, we previously reported relations between FA and saccadic latency in patients with schizophrenia and healthy controls (Manoach et al., 2007). In the present study, instead of examining relations of FA with behavior, we examined FA in relation to the latency visual responses as measured by MEG. By testing for relations in the entire brain, without making any assumptions about the anatomical connections between regions,

* Corresponding author. Massachusetts General Hospital, 149 13th Street, Room 2608, Charlestown, MA 02129, USA. Fax: +1 617 726 4078.
E-mail address: dara@nmr.mgh.harvard.edu (D.S. Manoach).
1 David S. Tuch's current address is Novartis Pharma AG, Basel, Switzerland.

Available online on ScienceDirect (www.Sciencedirect.com).

this method relates cortical function to the microstructural integrity of white matter tracts in an unbiased manner and can reveal white matter pathways that may contribute to inter-individual variability in the timing of neural activity. The visual responses were evoked by fixating a saccadic goal and were time-locked to the end point of the saccade. Post-saccadic visual responses may maximize timing variability since previous work demonstrates significantly greater variability in visual responses in V1 neurons following fixational saccadic eye movements compared to relatively steady fixation (Gur et al., 1997; Martinez-Conde et al., 2000). Since early visual responses are influenced by modulatory top-down signals (Moore and Armstrong, 2003; Ruff et al., 2006), we hypothesized that inter-individual differences in the conduction velocity of fibers from modulatory areas would contribute to variation in response latency. Thus, our aim was to identify regions that may modulate early visual responses by correlating FA with the timing of the peak early visual response. More generally, this method can be applied to investigate the contribution of white matter microstructural integrity to variability in the latencies of EEG or MEG evoked responses non-invasively in human subjects.

Experimental procedures

Participants

Eight healthy young adults (4 male; mean age: 22±2) participated. We restricted our sample to young subjects within a restricted range of ages given the documented relation of increasing age with decreasing FA (Pfefferbaum et al., 2000; Salat et al., 2005). All subjects gave written informed consent. The study was approved by the Human Research Committee at Massachusetts General Hospital and adhered to the principles of the Declaration of Helsinki.

Magnetoencephalography acquisition and eye movement measurements

Whole head MEG signals (102 magnetometers, 204 planar gradiometers) were recorded in a magnetically shielded room (IMEDCO, Hagendorf, Switzerland) using a dc-SQUID Neuromag™ VectorView system (Elekta-Neuromag, Helsinki, Finland). The data were filtered to a 0.1–200 Hz bandpass and sampled at 600 Hz. To allow registration of MEG and MRI data, the sites of four head-position indicator (HPI) coils that were attached to the scalp were digitized using a 3Space Fastrak digitizer (Polhemus, Colchester, VT, USA) integrated with the Vectorview system. The horizontal and vertical components of eye movements were recorded concurrently with MEG, using two pairs of bipolar electro-oculogram (EOG) electrodes.

Saccadic task

Fig. 1 provides a graphic depiction of the task and a description of task parameters. During MEG acquisition, participants performed a saccadic task. Visual stimuli were generated using the Vision Shell programming platform (www.vision shell.com) and presented with a Digital Light Processing (DLP)
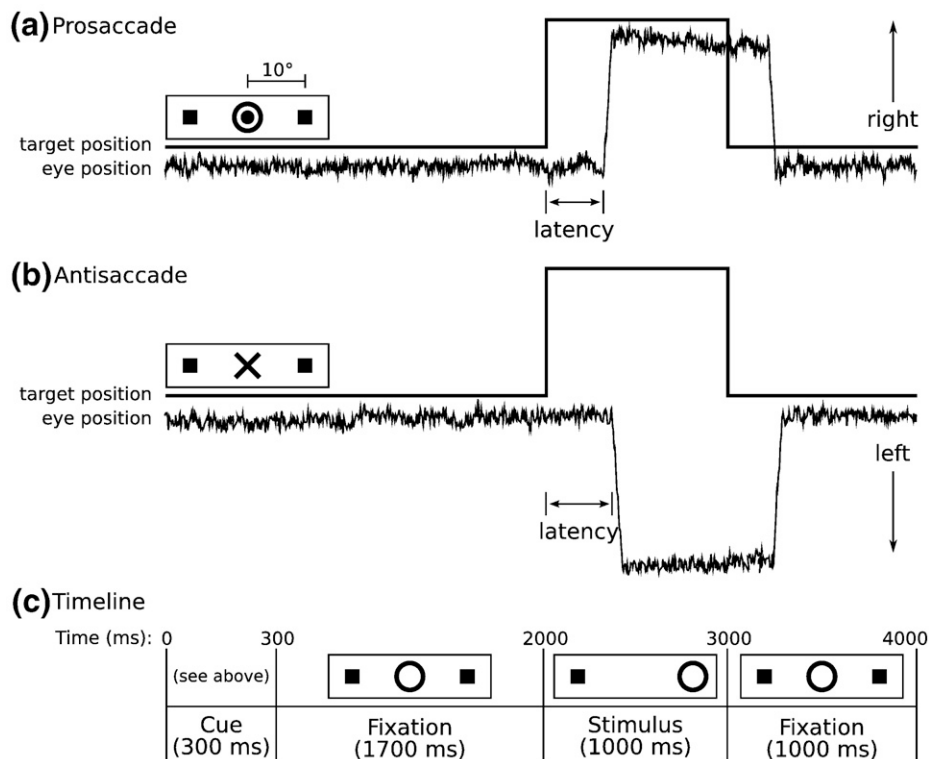

Fig. 1. Saccadic paradigm. Saccadic trials lasted 4000 ms and began with an instructional cue at screen center. For half of the participants, an orange ring was the cue for a PS trial and a blue X the cue for an AS trial. These cues were reversed for the rest of the participants. The cue was flanked horizontally by two small green squares of 0.2° side that marked the potential locations of stimulus appearance, 10° left and right of center. These squares remained on the screen for the duration of each run. At 300 ms the instructional cue was replaced by a green fixation ring at screen center with a diameter of 0.4° and luminance of 20 cd/m². After 1700 ms the ring shifted to one of the two stimulus locations, right or left, with equal probability. This ring was the stimulus to which participants responded. The green ring remained in the peripheral location for 1000 ms and then returned to the center where participants were instructed to return their gaze for 1000 ms. Fixation intervals were simply a continuation of the fixation display that constituted the final second of the previous saccadic trial.

InFocus 350 projector, through an opening in the wall, onto a back-projection screen placed 102 cm in front of the participant inside the magnetically shielded room. Each participant performed eight runs of the saccadic task with short breaks in between. Each run was 5 min 22 s and consisted of a pseudorandom sequence of prosaccade, antisaccade, and fixation trials. Prosaccade trials required participants to make a saccade to a suddenly appearing visual stimulus, and antisaccade trials required participants to make a saccade in the opposite direction, to a stimulus that remained on the screen for the duration of the experiment. The saccadic trials were balanced for right and leftward movements and lasted 4000 ms. The total experiment lasted approximately 1 h and generated a total of 278 prosaccade, 285 antisaccade, and 107 fixation trials.

MRI and DTI acquisition

Images were collected using a 3.0 T Siemens Trio MRI scanner (Siemens Medical System, Iselin, NJ). Two T1-weighted high-resolution structural images were acquired in the sagittal plane for slice prescription, spatial normalization, and cortical surface reconstruction using a high-resolution 3D magnetization prepared rapid gradient echo (MP-RAGE) sequence (repetition time (TR), 2530 ms; echo spacing, 7.25 ms; echo time (TE), 3 ms; flip angle 7°) with an in-plane resolution of 1.3 mm and 1 mm slice thickness.

Single-shot EPI DTI data were acquired using a twice-refocused spin echo sequence (Reese et al 2003). The sequence parameters were repetition time (TR)=8400 ms, echo time
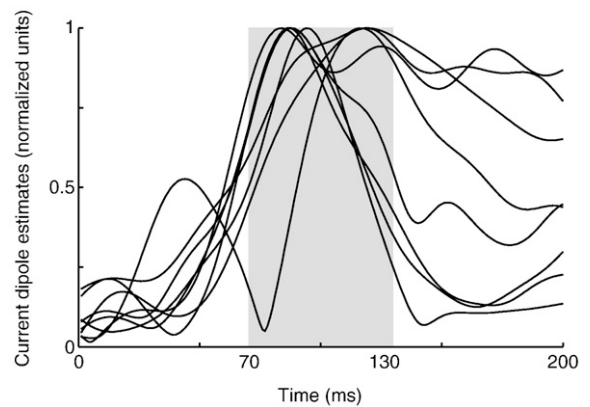
Fig. 3. Current dipole estimates as a function of time for each participant in normalized units. The latencies of peaks between 70 and 130 ms (shaded area) from the saccade end point were measured.

(TE)=82 ms, b=700 s/mm^2, NEX=1, 72 diffusion directions; 128×128 matrix; 2×2 mm in-plane resolution; 64 axial oblique (AC–PC) slices; 2 mm (0 mm gap) slice thickness, scan duration 12'44. The n=72 diffusion directions were obtained using the electrostatic shell algorithm (Jones, 2004). The slices were oriented in the intercommissural (AC–PC) plane. The eddy current distortions between diffusion weightings were typically less than two voxels.

Analysis of eye movement data

The EOG data were low-pass filtered at 30 Hz and scored in MATLAB (Mathworks, Natick, MA) using a partially automated program that determined the directional accuracy of each saccade with respect to the required response, the latency of saccadic initiation, and the endpoint of the saccade. For each trial, saccadic onset was defined as the point preceding peak velocity at which the horizontal eye-position trace deviated from fixation (Fig. 2). To determine this point an automated algorithm started at the point of peak velocity and searched the eye-position trace backwards to fixation. The endpoint of the saccade was defined as the point following peak velocity at which the eye reached fixation. Fixation was defined as the time point at which the slope of the eye-position trace was zero as determined by evaluating the slope in relation to the surrounding time points, a moving window of 5 ms. Algorithm results were visually inspected to ensure accuracy. Only trials with saccades in the desired direction and latencies between 130 and 800 ms were considered correct, and only correct saccades were included in the regression analysis. The cutoff of 130 ms excluded anticipatory saccades, which are executed too quickly to be a valid response to the appearance of the target (Doricchi et al., 1997; Fischer and Breitmeyer, 1987; Straube et al., 1999).

MEG analysis

MEG data were bandpass filtered at 0.1–30 Hz. Consistently noisy channels were identified by visual inspection and omitted from analysis. Each participant's waveforms were averaged to the endpoint of the saccade. Only trials meeting amplitude criteria (maximum peak-to-peak amplitude; magnetometers: 10,000 fT, gradiometers: 3000 fT/cm) were included in the averaged waveforms. A 200 ms interval prior to the beginning of each trial was used as a baseline and
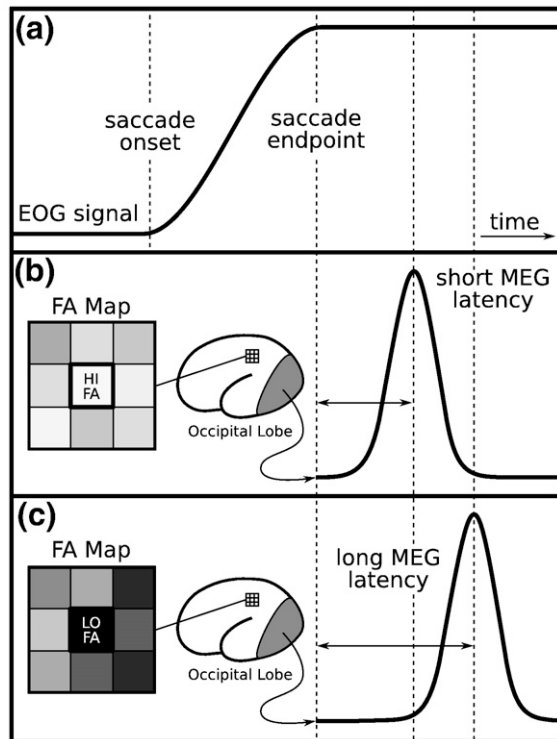
Fig. 2. Schematic illustration of method and findings: (a) Idealized trace of the horizontal eye-position over time with saccade onset and endpoint indicated. The latency measure was the timing of the peak occipital MEG evoked response occurring between 70 and 130 ms following the saccade endpoint. (b, c) Schematic illustrations of FA values in a grid of voxels in subcortical white matter regions that were correlated with the latency of the peak MEG evoked visual response in occipital cortex. (b) High FA values correspond to short latencies and (c) low FA values correspond to long latencies.

subtracted from each epoch before the trial was added to the average. For source estimation, a 3D structural image was created for each participant by averaging the two MP-RAGE scans after correcting for motion. The structural image was segmented and inflated using FreeSurfer software (Dale et al., 1999; Fischl et al., 1999). The source space for MEG analysis was seeded onto the cortical surface using approximately 3000 dipolar current sources per hemisphere. The forward solution was calculated using a single-compartment boundary element model (Hamalainen and Sarvas, 1989) with the inner skull surface segmented from MRI data. An L2 minimum norm estimate with noise-normalization was applied to the averaged MEG signals, yielding dynamic statistical parametric maps (dSPM) (Dale et al., 2000; Hamalainen and Ilmoniemi,
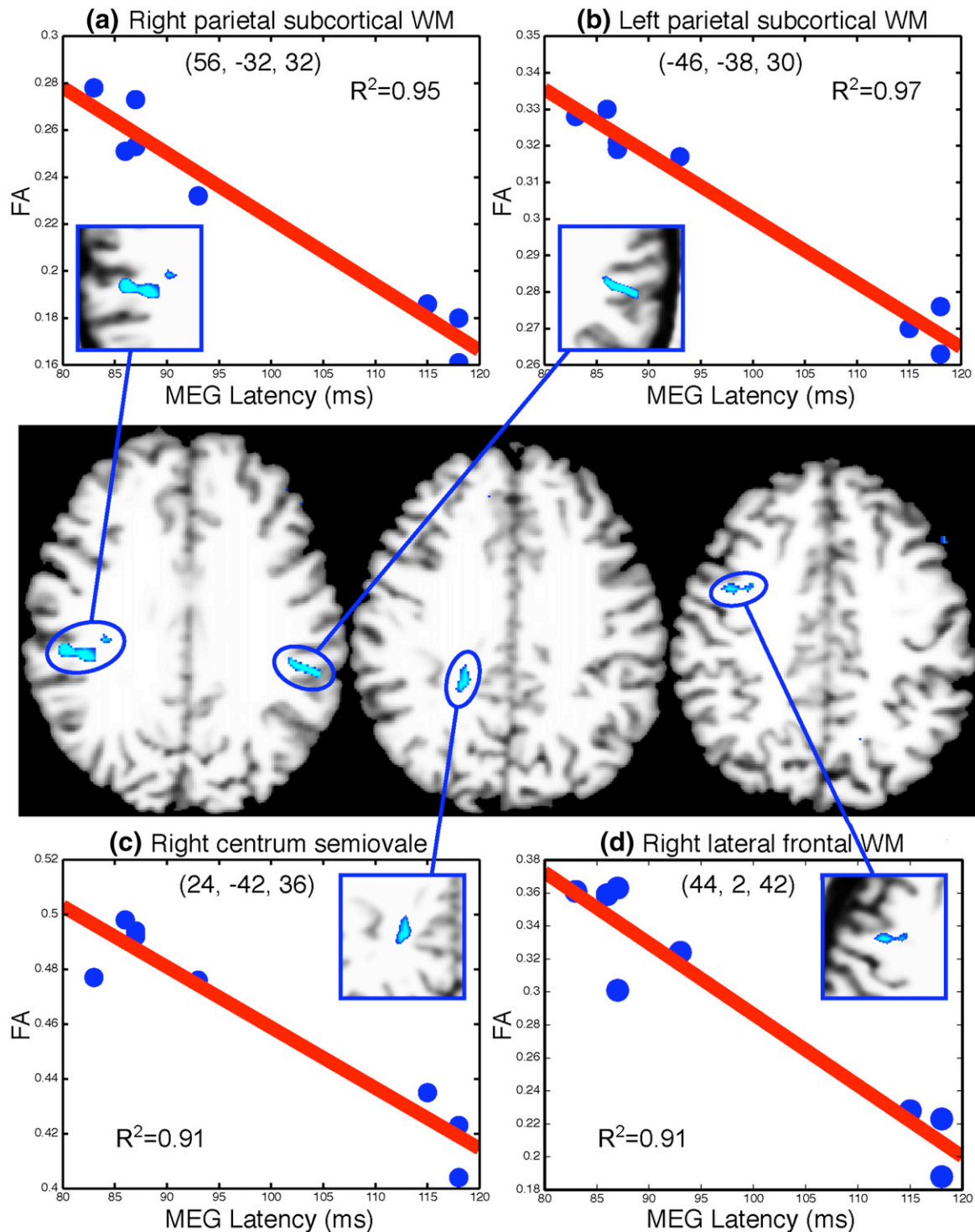
Fig. 4. Regions showing significant FA-latency correlations with scatter plots. Statistical maps are displayed at $p \leq 0.001$ on horizontal slices of an MNI-normalized representative T1 volume. (a–d) Scatter plots of FA and MEG latency with regression lines and R-squared values for bilateral parietal, right lateral frontal, and right centrum semiovale maxima. Talairach coordinates for the voxel of maximum correlation are provided (x, y, z). Approximate dimensions of each region of correlation in the group map in mm are lateral parietal: right: 18×6×4 mm; left: 16×6×8 mm; right centrum semiovale: 6×12×6 mm; right lateral frontal: 12×8×6 mm. WM=white matter.

1984). In calculating the average dipole waveforms, the dipole orientation was approximately constrained to the cortical normal direction by setting source variances for the transverse current components to be 0.4 times the variance of the currents normal to the cortical surface (Lin et al., 2006a; Lin et al., 2006b).

We considered data from prosaccade and antisaccade trials separately and also averaged them to derive latency measures. The maximum dSPM activation within 70–130 ms following the end of the saccade (re-fixation on the saccadic goal) was identified within the occipital cortex of each hemisphere. The latency of the neuromagnetic visual response for each participant was derived from the occipital vertex with the maximum response in either hemisphere.

DTI preprocessing

Raw diffusion data were corrected for head motion and residual eddy current distortion by registering all images to the first acquired T2 image. Using the FLIRT tool (Jenkinson and Smith, 2001) with a 12-df global affine transformation, the DTI images were registered using a mutual information cost function, available through the FSL software library (www.fmrib.ox.ac.uk/fsl). Trilinear interpolation was used for the resampling. Inter-subject registration of individual FA maps to the Montreal Neurological Institute (MNI305) atlas (Collins et al., 1994) was performed using the average of the two 3D structural images. The resulting transformation was applied to individual FA volumes. The MNI-normalized FA volumes were smoothed with a 3D Gaussian kernel with 6-mm full-width at half-maximum (FWHM) and 6-mm spatial extent. Voxels with trace diffusion>6 μm^2/ms were not included in the smoothing operation in an effort to minimize the partial volume contribution from cerebrospinal fluid. FA was calculated for each voxel using in-house software.

FA-Latency regression analysis

FA values were regressed on the peak MEG latency for each voxel in whole-brain FA volume. To correct the regression map for multiple comparisons, we ran 10,000 Monte Carlo simulations of the smoothing, averaging, and resampling parameters of the regression data using synthesized white Gaussian noise data. This determines the likelihood that a cluster of a certain size would be found by chance for our starting threshold of $p \leq 0.001$ and yields a corrected p-value ≤0.05. Significant clusters are visualized as an overlay on horizontal slices of a representative MNI-normalized individual T1 volume (Fig. 4). MNI coordinates for the voxel with the maximum correlation within each cluster were transformed to standard Talairach space using an algorithm developed by Matthew Brett (http://imaging.mrc-cbu.cam.ac.uk/imaging/MniTalairach).

Results

The latencies of the peak of the earliest MEG evoked responses to the saccadic target in occipital lobe were almost identical for prosaccade and antisaccade trials and yielded similar correlations with FA, so we present only the analyses that used the combined data. Fig. 3 presents the current dipole estimates from which latency measurements were derived for each participant. These show a range of latencies for the peak

response within the 70 to 130 ms time window. As displayed in Fig. 4, FA was significantly related to the latency of the occipital MEG evoked response ($p \leq 0.001$ uncorrected; $p \leq 0.05$ corrected for multiple comparisons) in the right centrum semi-ovale (24, −42, 36) and in white matter regions at or near the gray-white border of the lateral parietal cortex bilaterally (right: 56, −32, 32; left: −46, −38, 30) and the right lateral frontal cortex near the middle and inferior frontal gyri (44, 2, 42).

To determine whether the correlated regions lay in white matter for each participant, we overlaid the significant cluster on the averaged high-resolution anatomical scan for each participant. With the exception of the centrum semiovale, which lay entirely in white matter for all participants, the more superficial subcortical regions contained voxels in both gray and white matter. To rule out partial average volume effects (due to voxels that either spanned gray and white matter or fell in entirely in gray matter for only some participants) as accounting for our results, we conducted the correlations with latency using only voxels that lay entirely in white matter. To this end, we segmented each participant's high-resolution anatomical scan into gray and white matter using FreeSurfer software (Fischl et al., 2002) and overlaid the regions of significant correlation from the averaged group data. Within each region, an average FA value was calculated for each participant using only the voxels that lay entirely in white matter. Using these FA values, the correlations of FA with latency of the MEG evoked response remained significant in all of the regions identified: lateral parietal cortex bilaterally (right: $R^2 = 0.91$, $p < 0.01$; left: $R^2 = 0.86$, $p < 0.01$) and right lateral frontal cortex ($R^2 = .89$, $p < 0.01$).

Discussion

Across individuals, faster latencies of peak evoked neuromagnetic fields in occipital cortex were related to greater FA in areas thought to contain fibers from cortical regions that modulate early visual responses: posterior parietal cortex and frontal eye field (FEF). We interpret these relations to reflect that white matter fibers linking these ocular motor regions to early visual regions transmit information that modulates the visual response, and that the speed of transmission depends on white matter properties, such as myelination and axon diameter, that contribute to FA (Waxman, 1980). Increased myelination would correspond to increased conduction velocity in fibers from top-down regions and thus a reduced latency of the visual evoked response. While there are prior reports of relations between FA and physiological measures such as the amplitude of steady-state visual evoked potentials (Butler et al., 2005), measures of functional connectivity (Boorman et al., 2007), and task-related BOLD signal (Baird et al., 2005; Olesen et al., 2003), this is the first report of relations between FA and the *timing* of evoked responses. Although it will be important to validate these findings with larger samples and well-established visual paradigms, these relations suggest that biophysical properties of white matter affect the timing of early visual responses. More importantly, this preliminary report demonstrates a non-invasive method to relate the timing information from evoked-response experiments to the biophysical properties of white matter measured with DTI using a whole-brain approach.

Factors that may contribute to individual differences in white matter physiology among healthy individuals are largely

unknown, but likely include gene expression (Michailov et al., 2004). Individual differences in white matter physiology, particularly myelination have been proposed to contribute to variation in information processing speed (Luciano et al., 2004) consistent with recent reports of correlations between FA and cognitive reaction time (Bucur et al., 2007; Gold et al., 2007; Madden et al., 2004; Manoach et al., 2007; Nestor et al., 2007; Tuch et al., 2005; Westerhausen et al., 2006). Here we report relations between FA and the latency of evoked neural responses, which are presumably more proximal measures of neuronal function than are measures of the latency of behavior. These relations may be based on the speed of axonal transmission from frontal and parietal regions that modulate early visual responses.

Classic peaks in event-related potentials such as the P1, P170 and N200 are thought to arise from sources within the occipital, parietal, and temporal lobes due to sensory and intermediate levels of processing. The neuromagnetic responses in this study originated in the occipital lobe and may represent an equivalent of the P100 or P1 m component of the visual evoked response, in our case representing a response to foveating a stimulus following a saccade. Early visual responses are usually measured in response to a stimulus appearing in foveal vision during fixation. The standard deviation of the peak latency for early visual responses is approximately 15 ms, with some dependence on the experimental design (Fahle and Bach, 2006). Variability in the latency of early visual responses has been attributed to small saccadic eye movements that occur during fixation (Gur et al., 1997; Martinez-Conde et al., 2000). Since fixational microsaccades and longer-range saccades rely on overlapping circuitry, we reasoned that longer-range saccades might also give rise to variability of visual responses both within and across individuals. In the present study the latency of the evoked magnetic responses ranged from 83 to 118 ms and there was a division between participants showing short vs. long latencies (see plots in Fig. 2). While a larger sample might have produced a more continuous distribution of latencies, the division in latency may also reflect that the visual responses from short and long latency participants arose from different occipital regions. The limited spatial resolution of our MEG source modeling approach does not allow us to exclude this explanation of our findings. However, if this were the case, we would not expect to see strong and specific inverse correlations between the latency of these visual responses and FA in the white matter presumed to underlie top-down ocular motor regions.

Although plausible, the explanation of top-down modulation of the timing of early visual responses rests on the presumption that the correlated areas contain fibers that originate in posterior parietal cortex and FEF and synapse in early visual areas, which is not something that we can demonstrate using these techniques. For example, we hypothesize that the right frontal region showing a significant correlation contains fibers from FEF. The putative human homologue of FEF is located in the vicinity of the precentral sulcus and gyrus (Koyama et al., 2004; Paus, 1996) with distinct regions in the superior and inferior portions (Luna et al., 1998; Simo et al., 2005). While it is possible that the region showing a correlation contains fibers from FEF, we cannot definitively pinpoint fiber origins or endpoints. The correlated region in the deep white matter of right centrum semiovale is even less regionally specific. While the centrum semiovale contains major white matter fascicles from frontal and parietal cortex, whether the region identified by the correlation analysis carries fibers from ocular motor

regions is impossible to determine in the present study. While DTI-based tractography may provide suggestive evidence of fiber origins and endpoints, it requires numerous assumptions regarding crossing fibers and the location and size of seed regions. An advantage of the present technique is that it makes no such assumptions, rather it examines relations of latency to FA in the entire brain. In the present study the findings were regionally specific in that they lay in regions that could plausibly contain fibers from ocular motor regions.

Although the anatomy of white matter in humans is not well established (c.f., Schmahmann et al 2007), extensive anatomical connections between FEF, lateral intraparietal area (LIP), and occipital areas have been documented in monkeys (Andersen et al., 1990; Blatt et al., 1990; Cavada and Goldman-Rakic, 1989). Moreover, electrical stimulation of macaque FEF neurons modulates activity in V4 neurons (Moore and Armstrong, 2003). There is also evidence of top-down modulation of occipital responses in humans. Transcranial magnetic stimulation of FEF modulates both fMRI visual responses in early human retinotopic cortex (areas V1–V4) (Ruff et al., 2006) and event-related potentials (ERPs) recorded from occipital electrodes (Taylor et al., 2007). When applied to right posterior parietal cortex during visual search, transcranial magnetic stimulation eliminates the early phase of N2pc, an ERP generated in occipital lobe (Fuggetta et al., 2006). Finally, patients with lesions of right parietal cortex show abnormal fMRI visual responses in areas V1–V4, but only under conditions of increased attentional load, suggesting a failure of top-down attentional modulation of visual responses (Vuilleumier and Driver, 2007). These findings suggest that anatomical connections exist between FEF and posterior parietal cortex and early visual regions that may modulate both early and later visual responses.

It should be emphasized that some of the voxels in the correlated clusters contained gray matter. We chose not to restrict our analyses to deep subcortical white matter as it excludes white matter close to the gray-white border that emanates from specific regions, such as subcortical U-fibers. An important advantage of conducting the analysis in the whole volume is that meaningful, regionally specific correlations in these border areas can be detected. A disadvantage of sampling close to the gray-white border in a group analysis is that it results in partial average volume effects due to voxels that either span gray and white matter or that fall entirely in gray matter for only some participants given variations in cortical anatomy. The presence of gray matter in the correlated regions does not necessarily invalidate the results. Gray matter also contains myelinated fiber tracts that could contribute to the speed of neural conduction. However, since our FA values likely varied across individuals depending on how much gray matter was included, partial volume averaging represents a potential confound in our analyses. In control analyses, we were able to exclude partial volume effects as an account of our findings. Specifically, when we measured averaged FA values in individual participants based on voxels that lay entirely in white matter, the correlations with latency remained significant.

In conclusion, we observed relations between FA in parietal and frontal white matter and the latency of the MEG visual response in occipital cortex time-locked to arrival at a saccadic goal. These preliminary results suggest that the microstructural integrity of white matter connecting top-down cortical regions to early visual areas contributes to inter-individual variability of the timing of visual evoked responses. More

generally, we introduce a non-invasive method that can illuminate the contribution of white matter physiology to inter-individual variability in the latency of evoked potentials in health and in neuropathologic conditions.

Acknowledgments

References

Andersen, R.A., Asanuma, C., Essick, G., Siegel, R.M., 1990. Corticocortical connections of anatomically and physiologically defined subdivisions within the inferior parietal lobule. J. Comp. Neurol. 296, 65–113.

Baird, A.A., Colvin, M.K., Vanhorn, J.D., Inati, S., Gazzaniga, M.S., 2005. Functional connectivity: integrating behavioral, diffusion tensor imaging, and functional magnetic resonance imaging data sets. J. Cogn. Neurosci. 17, 687–693.

Beaulieu, C., 2002. The basis of anisotropic water diffusion in the nervous system — a technical review. NMR Biomed. 15, 435–455.

Blatt, G.J., Andersen, R.A., Stoner, G.R., 1990. Visual receptive field organization and cortico-cortical connections of the lateral intraparietal area (area LIP) in the macaque. J. Comp. Neurol. 299, 421–445.

Boorman, E.D., O'Shea, J., Sebastian, C., Rushworth, M.F., Johansen-Berg, H., 2007. Individual differences in white-matter microstructure reflect variation in functional connectivity during choice. Curr. Biol. 17, 1426–1431.

Bucur, B., Madden, D.J., Spaniol, J., Provenzale, J.M., Cabeza, R., White, L.E., Huettel, S.A., 2008. Age-related slowing of memory retrieval: contributions of perceptual speed and cerebral white matter integrity. Neurobiol. Aging 29, 1070–1079.

Butler, P.D., Zemon, V., Schechter, I., Saperstein, A.M., Hoptman, M.J., Lim, K.O., et al., 2005. Early-stage visual processing and cortical amplification deficits in schizophrenia. Arch. Gen. Psychiatry 62, 495–504.

Cavada, C., Goldman-Rakic, P.S., 1989. Posterior parietal cortex in rhesus monkey: II. Evidence for segregated corticocortical networks linking sensory and limbic areas with the frontal lobe. J. Comp. Neurol. 287, 422–445.

Collins, D.L., Neelin, P., Peters, T.M., Evans, A.C., 1994. Automatic 3D intersubject registration of MR volumetric data in standardized Talairach space. J. Comput. Assist. Tomogr. 18, 192–205.

Dale, A.M., Fischl, B., Sereno, M.I., 1999. Cortical surface-based analysis. I. Segmentation and surface reconstruction. Neuroimage 9, 179–194.

Dale, A.M., Liu, A.K., Fischl, B.R., Buckner, R.L., Belliveau, J.W., Lewine, J.D., Halgren, E., 2000. Dynamic statistical parametric mapping: combining fMRI and MEG for high-resolution imaging of cortical activity. Neuron 26, 55–67.

Doricchi, F., Perani, D., Inoccia, C., Grassi, F., Cappa, S.F., Bettinardi, V., et al., 1997. Neural control of fast-regular saccades and antisaccades: an investigation using positron emission tomography. Exp. Brain Res. 116, 50–62.

Fahle, M., Bach, M., 2006. Origin of the VEP potentials, In: Heckenlively, J.R., Arden, G.B. (Eds.), Principles and Practice of Clinical Electrophysiology of Vision, 2nd Edition. Cambridge, MA, MIT Press, pp. 207–234.

Fischer, B., Breitmeyer, B., 1987. Mechanisms of visual attention revealed by saccadic eye movements. Neuropsychologia 25, 73–83.

Fischl, B., Salat, D.H., Busa, E., Albert, M., Dieterich, M., Haselgrove, C., et al., 2002. Whole brain segmentation: automated labeling of neuroanatomical structures in the human brain. Neuron 33, 341–355.

Fischl, B., Sereno, M.I., Dale, A.M., 1999. Cortical surface-based analysis. II. Inflation, flattening, and a surface-based coordinate system. Neuroimage 9, 195–207.

Fuggetta, G., Pavone, E.F., Walsh, V., Kiss, M., Eimer, M., 2006. Cortico-cortical interactions in spatial attention: a combined ERP/TMS study. J. Neurophysiol. 95, 3277–3280.

Gold, B.T., Powell, D.K., Xuan, L., Jiang, Y., Hardy, P.A., 2007. Speed of lexical decision correlates with diffusion anisotropy in left parietal and frontal white matter: evidence from diffusion tensor imaging. Neuropsychologia 45, 2439–2446.

Gur, M., Beylin, A., Snodderly, D.M., 1997. Response variability of neurons in primary visual cortex (V1) of alert monkeys. J. Neurosci. 17, 2914–2920.

Hamalainen, M.S., Ilmoniemi, R., 1984. Interpreting Measured Magnetic Fields of the Brain: Estimates of Current Distribution. University of Technology, Dept. of Technical Physics Report, Helsinki, pp. TKK–F-A559.

Hamalainen, M.S., Sarvas, J., 1989. Realistic conductivity geometry model of the human head for interpretation of neuromagnetic data. IEEE Trans. Biomed. Eng. 36, 165–171.

Harsan, L.A., Poulet, P., Guignard, B., Steibel, J., Parizel, N., de Sousa, P.L., et al., 2006. Brain dysmyelination and recovery assessment by noninvasive in vivo diffusion tensor magnetic resonance imaging. J. Neurosci. Res. 83, 392–402.

Jenkinson, M., Smith, S., 2001. A global optimisation method for robust affine registration of brain images. Med. Image Anal. 5, 143–156.

Jones, D.K., 2004. The effect of gradient sampling schemes on measures derived from diffusion tensor MRI: a Monte Carlo study. Magn. Reson. Med. 51, 807–815.

Koyama, M., Hasegawa, I., Osada, T., Adachi, Y., Nakahara, K., Miyashita, Y., 2004. Functional magnetic resonance imaging of macaque monkeys performing visually guided saccade tasks: comparison of cortical eye fields with humans. Neuron 41, 795–807.

Lin, F.H., Belliveau, J.W., Dale, A.M., Hamalainen, M.S., 2006a. Distributed current estimates using cortical orientation constraints. Hum. Brain Mapp. 27, 1–13.

Lin, F.H., Witzel, T., Ahlfors, S.P., Stufflebeam, S.M., Belliveau, J.W., Hamalainen, M.S., 2006b. Assessing and improving the spatial accuracy in MEG source localization by depth-weighted minimum-norm estimates. Neuroimage 31, 160–171.

Luciano, M., Wright, M.J., Geffen, G.M., Geffen, L.B., Smith, G.A., Martin, N.G., 2004. A genetic investigation of the covariation among inspection time, choice reaction time, and IQ subtest scores. Behav. Genet. 34, 41–50.

Luna, B., Thulborn, K.R., Strojwas, M.H., McCurtain, B.J., Berman, R.A., Genovese, C.R., Sweeney, J.A., 1998. Dorsal cortical regions subserving visually guided saccades in humans: an fMRI study. Cereb. Cortex 8, 40–47.

Madden, D.J., Whiting, W.L., Huettel, S.A., White, L.E., MacFall, J.R., Provenzale, J.M., 2004. Diffusion tensor imaging of adult age differences in cerebral white matter: relation to response time. Neuroimage 21, 1174–1181.

Manoach, D.S., Ketwaroo, G.A., Polli, F.E., Thakkar, K.N., Barton, J.J., Goff, D.C., et al., 2007. Reduced microstructural integrity of the white matter underlying anterior cingulate cortex is associated with increased saccadic latency in schizophrenia. Neuroimage 37, 599–610.

Martinez-Conde, S., Macknik, S.L., Hubel, D.H., 2000. Microsaccadic eye movements and firing of single cells in the striate cortex of macaque monkeys. Nat. Neurosci. 3, 251–258.

Michailov, G.V., Sereda, M.W., Brinkmann, B.G., Fischer, T.M., Haug, B., Birchmeier, C., et al., 2004. Axonal neuregulin-1 regulates myelin sheath thickness. Science 304, 700–703.

Moore, T., Armstrong, K.M., 2003. Selective gating of visual signals by microstimulation of frontal cortex. Nature 421, 370–373.

Nestor, P.G., Kubicki, M., Spencer, K.M., Niznikiewicz, M., McCarley, R.W., Shenton, M.E., 2007. Attentional networks and cingulum bundle in chronic schizophrenia. Schizophr. Res. 90, 308–315.

Olesen, P.J., Nagy, Z., Westerberg, H., Klingberg, T., 2003. Combined analysis of DTI and fMRI data reveals a joint maturation of white and grey matter in a fronto-parietal network. Brain Res. Cogn. Brain Res. 18, 48–57.

Paus, T., 1996. Location and function of the human frontal eye-field: a selective review. Neuropsychologia 34, 475–483.

Pfefferbaum, A., Sullivan, E.V., Hedehus, M., Lim, K.O., Adalsteinsson, E., Moseley, M., 2000. Age-related decline in brain white matter anisotropy measured with spatially corrected echo-planar diffusion tensor imaging. Magn. Reson. Med. 44, 259–268.

Reese, T.G., Heid, O., Weisskoff, R.M., Wedeen, V.J., 2003. Reduction of eddy-current-induced distortion in diffusion MRI using a twice-refocused spin echo. Magn. Reson. Med. 49, 177–182.

Ruff, C.C., Blankenburg, F., Bjoertomt, O., Bestmann, S., Freeman, E., Haynes, J.D., et al., 2006. Concurrent TMS-fMRI and psychophysics reveal frontal influences on human retinotopic visual cortex. Curr. Biol. 16, 1479–1488.

Salat, D.H., Tuch, D.S., Greve, D.N., van der Kouwe, A.J., Hevelone, N.D., Zaleta, A.K., et al., 2005. Age-related alterations in white matter microstructure measured by diffusion tensor imaging. Neurobiol. Aging 26, 1215–1227.

Schmahmann, J.D., Pandya, D.N., Wang, R., Dai, G., D'Arceuil, H.E., de Crespigny, A.J., Wedeen, V.J., 2007. Association fibre pathways of the brain: parallel observations from diffusion spectrum imaging and autoradiography. Brain 130, 630–653.

Simo, L.S., Krisky, C.M., Sweeney, J.A., 2005. Functional neuroanatomy of anticipatory behavior: dissociation between sensory-driven and memory-driven systems. Cereb. Cortex 15, 1982–1991.

Straube, A., Riedel, M., Eggert, T., Müller, N., 1999. Internally and externally guided voluntary saccades in unmedicated and medicated schizophrenic patients. Part I. Saccadic velocity. Eur. Arch. Psychiatry Clin. Neurosci. 249, 1–6.

Taylor, P.C., Nobre, A.C., Rushworth, M.F., 2007. FEF TMS affects visual cortical activity. Cereb. Cortex 17, 391–399.

Tuch, D.S., Salat, D.H., Wisco, J.J., Zaleta, A.K., Hevelone, N.D., Rosas, H.D., 2005. Choice reaction time performance correlates with diffusion anisotropy in white matter pathways supporting visuospatial attention. Proc. Natl. Acad. Sci. U. S. A. 102, 12212–12217.

Vuilleumier, P., Driver, J., 2007. Modulation of visual processing by attention and emotion: windows on causal interactions between human brain regions. Philos. Trans. R. Soc. Lond., B Biol. Sci. 362, 837–855.

Waxman, S.G., 1980. Determinants of conduction velocity in myelinated nerve fibers. Muscle Nerve 3, 141–150.

Westerhausen, R., Kreuder, F., Woerner, W., Huster, R.J., Smit, C.M., Schweiger, E., Wittling, W., 2006. Interhemispheric transfer time and structural properties of the corpus callosum. Neurosci. Lett. 409, 140–145.